Microbiology, Metabolites and Biotechnology
Journal home page: https://mmb.irost.ir
MMB
The former ARMMT

Polymicrobial Shifts in the Culturable Bacterial Microbiome Associated with Persian Oak Decline in Western Iran

Elahe Ahmadi[1, 2], Mojegan Kowsari[2]*, Davood Azadfar[1], Gholamreza Salehi Jouzani[2]

[1] *Department of Silviculture and Forest Ecology, Gorgan University of Agricultural Science and Natural Resources, Basij Square, P.O. Box: 4918943464, Gorgan, Iran.*
[2] *Microbial Biotechnology Department, Agricultural Biotechnology Research Institute of Iran (ABRII), Agricultural Research, Education and Extension Organization (AREEO), Karaj, Iran.*

Article Info

Document Type:
Research Paper

Received 04/08/2025
Received in revised form 06/12/2025
Accepted 19/12/2025

Published 19/12/2025

Keywords:
Cultivatable microbiome,
Endophytic bacteria,
Persian oak decline,
Polymicrobial disease

Abstract

Persian oak decline is a distinct syndrome within the broader oak decline complex observed in Iran, marked by excessive stem bleeding and larval galleries formed by the native buprestid beetle Agrilus hastulifer. To investigate this phenomenon, a comparative study was conducted on healthy and symptomatic trees across eight sites in Ilam province, western Iran. Culturable bacterial communities were identified using 16S rDNA sequencing. Symptomatic tissues from trees at Disease Index 5 yielded bacterial growth in 83.78% of samples—significantly higher than those from less affected trees. Bulk soil and rhizosphere samples also yielded greater bacterial yields than root, leaf, or stem tissues. Although bacterial community composition varied by site, diseased tissues consistently showed dominance of Enterobacteriaceae, while Bacillaceae and Moraxellaceae were more prevalent in healthy trees. Specific bacterial species, *Brenneria goodwinii, Serratia marcescens, and Brenneria roseae*, were strongly associated with diseased tissues, suggesting that necrosis was not due to random colonization. *Campylobacter jejuni* and an unidentified Clostridium taxon were frequently isolated from both healthy and diseased trees. These findings indicate a clear shift in the microbiome of diseased trees, with Enterobacteriaceae absent in healthy tissues. Crucially, no single dominant pathogen was identified, supporting the hypothesis that Persian oak decline is driven by a polymicrobial infection.

1. Introduction

Oak decline is a global, multifactorial syndrome characterized by progressive reductions in tree vigor, canopy thinning, branch dieback, and mortality, without a single identified causal agent (Denman *et al.*, 2018). Oak (*Quercus* spp.) forests dominate northern temperate hardwood regions and are ecologically and economically important (Gosling, 2024). Decline is associated with interacting abiotic stressors (e.g., drought, higher temperatures, and human activities) and biotic agents such as wood-boring insects, pathogenic fungi (e.g., *Biscogniauxia mediterranea and Diplodia corticola*), and bacteria (e.g., *Brenneria goodwinii*). These factors can act synergistically and accelerate dieback (Gosling *et al.*, 2024).

Climate change—particularly intensified winter–spring droughts—exacerbates physiological stress and increases susceptibility to pathogens (Nechita & Camarero, 2025; Gosling *et al.*, 2024). Since 2009, a chronic decline—especially of *Quercus brantii*—has affected Iran's Zagros forests. This decline reflects complex interactions among climatic stress, pathogens, and anthropogenic pressures, resulting in widespread canopy dieback, reduced regeneration, and ecosystem destabilization (Ahmadi *et al.*, 2014; Mehri *et al.*, 2024).

The Zagros forests (≈5 million ha, ~40% of Iran's forested area) provide key ecosystem services—biodiversity conservation, climate regulation, and watershed protection—and support roughly 10% of the national population (Sagheb-Talebi *et al.*, 2013). Oaks (primarily *Q. brantii*) cover over 90% of these forests and function as keystone species through acorn production and other ecological roles (Panahi *et al.*, 2012). Recent studies report substantial declines in *Q. brantii* due to interacting biotic and abiotic stressors, with severe dieback in central and southern provinces such as Ilam, Fars, Kohgiluyeh, and Lorestan (Bashiri & Abdollahzadeh, 2024; BakhshiGanje *et al.*, 2024; Gosling *et al.*, 2024). Key contributing factors include prolonged drought, rising temperatures, invasive pathogens, land-use change, and insect outbreaks (Gosling *et al.*, 2024). Human activities such as overgrazing and unsustainable logging have further intensified forest degradation (Mirhashemi *et al.*, 2023).

Affected trees commonly show bark cracking, necrotic lesions, stem and twig blight, bacterial ooze, discoloration, and evidence of wood-borer activity (Taghimollaei &

*Corresponding author E-mail: kowsari@abrii.ac.ir
DOI: 10.22104/mmb.2025.7777.1181
https://mmb.irost.ir/article_1620.html

Karamshahi, 2017). Similar decline symptoms have been reported in Britain and continental Europe and have often been linked to borer attacks and microbial pathogens (Denman *et al.*, 2014). Fungal pathogens are prominent contributors to oak decline worldwide. Canker-causing taxa such as *Biscogniauxia mediterranea*, *Diplodia corticola*, and *Discula quercina* have been associated with declining oaks, particularly in Mediterranean systems (Linaldeddu *et al.*, 2009). Other fungi, e.g., *Fusarium* spp., *Armillaria mellea*, and *Botryosphaeria* spp., have also been implicated in oak dieback in Mediterranean and Zagros forests (Mehri *et al.*, 2024; Jamali *et al.*, 2024). Although bacterial diseases of oak have been less studied historically, bacterial taxa such as *Xanthomonas*, *Pseudomonas*, *Rhodococcus*, and *Brenneria* have been identified as emerging contributors to oak decline, particularly under drought stress (Moradi-Amirabad *et al.*, 2019; Jamali *et al.*, 2024). In Iran, isolates including *Brenneria* spp., *Rahnella victoriana*, *Bacillus pumilus*, and *Stenotrophomonas maltophilia* have been reported from symptomatic trees (Moradi-Amirabad *et al.*, 2019; Ahmadi *et al.*, 2019). Given gaps in knowledge about bacterial roles, we conducted a systematic study to isolate cultivable bacteria from stems, roots, leaves, and soil of healthy and diseased *Q. brantii* West of Iran in 2015-2016. The aim was to compare cultivable community composition and identify candidate strains for pathogenicity testing (Mirhashemi *et al.*, 2022).

2. Materials and Methods

2.1. Materials

Nutrian Agar was prepared according to the standard formulation: 5 g beef extract, 10 g peptone, 5 g NaCl, and 15 g agar per liter of distilled water, adjusted to pH 7.0. For subsequent culturing, 5 mL LB broth was used per isolate, and the cultures were incubated overnight at 28–30 °C with shaking at 250 rpm. Sterile peptone water served both for soil resuscitation and for preparing serial tenfold dilutions. Soil aliquots were stored in sterile 1.5 mL microtubes (Eppendorf). Plant tissues were surface sterilized by immersion in 80% ethanol for 15 s, followed by 2% sodium NaOCl for 1–2 min, and rinsed three times with sterile distilled water.

Bacterial isolates were subjected to standard biochemical assays, including oxidase and catalase tests, nitrate reduction, pectin degradation using sodium polypectate, and protease activity. Carbohydrate fermentation ability was assessed using a panel of sugars (galactose, glucose, lactose, maltose, rhamnose, sucrose, fructose, xylose, glycerol, mannitol, and sorbitol). Additional characterization included oxidative/fermentative (O/F) reactions, Gram staining, and evaluation of fluorescent pigment production. All media and reagents were prepared according to standard microbiological protocols, and each assay was performed once without redundant descriptions in the revised text.

Genomic DNA was extracted using an SDS-based protocol (Zhou *et al.*, 1996). Amplification of the 16S rDNA region was performed with primers 27F and 1541R. Each PCR contained 0.2 U of Taq DNA polymerase (Thermo Fisher Scientific, USA) in a 30 µL reaction mixture, supplemented with 5 µL of 10× Taq buffer (Tris-HCl, pH 9.0, PCR enhancers, KCl, and 20 mM $MgCl_2$; Thermo Fisher Scientific) and a 10 mM dNTP mix.

2.2. Study site, investigation of symptoms, and sample collection

The composition of bacterial communities associated with oak tree tissues displaying disease symptoms, as well as those without symptoms, was investigated across eight distinct locations. In total, 120 trees were included in this study, from which 360 tissue samples and 240 soil samples were collected and processed.

The field survey was conducted in a noteworthy section of the Zagros forests between 2015 and 2016. This area is situated in Ilam province, where approximately 80% of oak trees have declined (Ilam encompasses 640,000 hectares of these forests) (33°38′15″N 46°25′22″E). Eight counties were specifically chosen to represent a diverse spatial distribution of symptomatic trees. According to field research, these eight habitats were the most affected by oak tree decline. Knowledge of the distribution of these symptomatic trees in western Iran was previously obtained through a project by the Forests, Range and Watershed Management Organization on oak decline in Iran (Forests, Range and Watershed Management Organization, 2013). The selected locations included: Arghavan (N33 39.709 E46 27.065), Saleh Abad (N33 32.458 E46 15.002), Tange Dalab (N33 41.935 E46 25.078), Chogha Sabz (N33 35.775 E46 26.497), Malek Shahi (N33 29.615 E46 29.700), Chavar (N33 41.120 E46 06.091), Eyvan (N33 46.148 E46 22.203), and Gale Jar (N33 43.122 E46 20.160). The progression of symptoms was evaluated using a decline index (DI) that ranged from 1 to 5. This index was determined based on symptom severity and the proportion of lesion or dead areas relative to the overall shoot length. The description of these symptoms was based on naturally infected samples. The DI categories were defined as follows: DI 1 indicated 1-10% damage, DI 2 indicated 10-30% damage, DI 3 indicated 30-60% damage, DI 4 indicated 60-90% damage, and DI 5 indicated 90-100% damage (as per González Alonso, 2009; Ishihara *et al.*, 2015).

Random samples were collected from three trees within each DI category at each of the eight selected locations. In total, 120 trees—both symptomatic and asymptomatic—were sampled (n = 120 trees). The symptomatic tissues comprised lesions at their advancing margins, wounds surrounding knots, regions showing resinosis, and wilting and yellowing of leaves. Although samples were not taken directly from larval galleries, observations of decline symptoms and the condition and formation of larval galleries were made during sampling.

Sampling was conducted in late spring, summer, and autumn over two consecutive years. In the first year, trees were tagged and their locations determined using GPS. The coded trees were revisited on each occasion for data recording, assessment of changes in tree condition, and sample collection. To isolate bacterial populations, samples were taken from three distinct tissues: stem (including sapwood and heartwood), leaf, and root, as well as soil (both bulk and rhizospheric soil) from each symptomatic and asymptomatic tree. Root samples were

obtained from buttress and feeder roots located at the base of the stem, at depths ranging from 5 to 15 cm. Stem, root, and leaf samples were excised and placed into plastic bags. The soil sampling approach involved collecting randomized samples from four separate areas within the plot (horizontal sampling) at a depth of 15 cm below the soil surface. Rhizospheric soil samples were specifically taken from a depth of 10 cm below the soil surface. The soil samples were manually homogenized through thorough physical mixing. All collected samples were sealed in new, unused polyethylene bags, kept at a cool temperature (4°C), and transported to the laboratory within 24 hours.

2.3. Sample Collection and Preparation for Bacterial Isolation

The stem (including both sapwood and heartwood), root, and leaf samples were collected and prepared following the protocols described by Biosca *et al.* (2003) and Sapp *et al.* (2016). During collection, sterile spades, clippers, and gloves were used. The spades and clippers were sterilized between samples from different individual plants to prevent cross-contamination. Roots were vigorously shaken to remove loose soil. Samples of stem, root, and leaf tissues (about 1 cm in length) were surface-sterilized by immersing them in 80% ethanol for 15 seconds, followed by treatment with 2% sodium hypochlorite solution for 1–2 minutes, and then rinsing them three times with sterile distilled water. Lastly, these tissue pieces were air-dried for 30 minutes.

For bacterial isolation, 1.9 grams of each sample was crushed in 20 milliliters of sterile water using a sterile mortar and pestle, as described by Trivedi *et al.* (2011). From the resulting suspension, approximately 100 µL was evenly spread across several culture plates containing NA. This medium was prepared according to the protocols of Jin *et al.* (2014), Schaad *et al.* (2001), and Ishihara *et al.* (2015).

Soil samples were homogenized in a sterile mortar, weighed, and distributed into 10 sterile Eppendorf microtubes, with 1 g in each. To resuscitate the bacterial species present in the soil, each aliquot was hydrated with 100 mL of sterile peptone water, thoroughly homogenized using magnetic stirring, and incubated at 32°C for 2 hours. After incubation, tenfold serial dilutions (1 ml of the initial suspension + 9 ml of sterile peptone water) were prepared from each aliquot. Due to the expected high level of bacterial contamination, six tenfold dilutions were performed for each soil sample. The fifth and sixth dilutions from each aliquot were completely filtered through 0.45 µm hydrophilic filters (Merck-Millipore®), and the filters were then inoculated onto the surface of Na (Merck®) solid culture medium and incubated at 32°C, as detailed by Constantin *et al.* (2016).

The cultures were incubated under aerobic conditions at room temperature for two to three weeks, with examinations every 2–3 days. When bacterial colonies appeared, they were subcultured by transferring them to fresh (NA). Subsequent subcultures were streaked onto NA plates to isolate single colonies, following the methods of Lelliot and Stead (1987). The isolated single colonies were checked for purity and grouped based on their colony morphology, cell shape, growth rate, and Gram staining characteristics.

2.4. DNA extraction, PCR amplification, and fungal and bacterial diversity analysis

Identification of bacterial strains from isolated single colonies was carried out by transferring the colonies into 5 ml of LB broth, using either a sterile pipette tip or an inoculating loop. These cultures were then incubated in a shaking (or stationary) incubator at 28–30°C and 250 rpm overnight (for more than 16 hours). DNA extraction from the bacterial cells was performed using the SDS-based method, following a modified version of the protocol described by Zhou *et al.* (1996).

For amplification of the 16S rDNA gene, primers 27F and 1541R were used, as outlined by Embarcadero-Jiménez *et al.* (2016). The PCR reaction mix included 1 µl of extracted DNA as the template, 10 pmol of each primer, 0.2 units of Taq polymerase (Thermo Fisher Scientific, USA), 5 µl of 10X Taq buffer (containing Tris-HCl pH 9.0, PCR enhancers, KCl, and 20 mM $MgCl_2$), and 10 mM dNTP mix (Thermo Fisher Scientific, USA). The final reaction volume was adjusted to 30 µl by adding sterile, purified water.

PCR amplification was conducted with the following thermal cycling conditions: an initial denaturation step at 95°C for 7 minutes, followed by 35 cycles of denaturation at 95°C for 50 seconds, annealing at 56°C for 1 minute, and extension at 72°C for 50 seconds. A final extension step was performed at 72°C for 5 minutes. The PCR products were then separated by electrophoresis on a 1% agarose gel using TAE buffer and visualized under UV light after staining with ethidium bromide.

The amplified PCR products were purified using a QIAquick PCR purification kit (Qiagen Inc., Chatsworth, CA, USA). Sequencing of the purified 16S rDNA products was performed using an ABI PRISM BigDye Terminator cycle sequencing ready reaction kit (Applied Biosystems, Foster City, CA, USA), following the manufacturer's instructions. The purified sequencing reactions were then run automatically on an Applied Biosystems model 377 automatic DNA sequencer

2.5. Data processing and statistical analysis of data

The presence of bacterial growth on the plated tissue pieces on agar was recorded. Differences in the percentage yield (calculated as the number of tissue pieces showing bacterial growth out of the total number plated) between healthy and symptomatic tissues were analyzed using a Generalized Linear Model (GLM) with a binomial error distribution and a logit link function, implemented in SPSS 20.0 (IBM North America, New York, USA), following Denman *et al.* (2016). For sequence identification, the BLAST tool from NCBI GenBank was used. Sequences with greater than 97% similarity were assigned to the same species. To assess variability in the composition of endophyte communities across the eight study sites, different disease development stages (based on disease index), and plant parts (roots versus aerial organs and soil), a permutational analysis of variance (PERMANOVA) was performed with 9999 permutations, using Bray-Curtis

dissimilarities. This analysis was done with the vegan package (Oksanen *et al.*, 2013). To visualize similarities in bacterial species composition across plots, a multidimensional scaling (MDS) analysis was conducted using the metaMDS function (Oksanen *et al.*, 2016). MDS is an ordination technique that aims to reduce the complexity of multidimensional data (in this case, plot species composition) into a lower-dimensional space while preserving the rank order of distances between points. Points located closer together on the plot represent samples with more similar species compositions, whereas points farther apart indicate greater differences (Minchin, 1987).

Additionally, an Analysis of Similarities (ANOSIM) was conducted, based on 999 permutations, to test whether bacterial communities differed significantly between sample types or sampling sites. To incorporate taxonomic data, we applied Canonical Correspondence Analysis (CCA), a direct-gradient ordination technique that relates environmental factors to species assemblages (Hall & Smol, 1992). Unlike methods based on Euclidean distances, CCA does not assume linear community trends and is therefore well-suited for studying community dynamics (Amaral-Zettler *et al.*, 2010). The first two axes (CCA1 and CCA2) usually account for most of the explained variation, with all axes constrained to represent linear combinations of ecological variables that maximize taxon dispersion across the ordination space (Hall and Smol, 1992).

3. Results and Discussion

3.1. Identification and phylogenetic analyses of endophytic bacteria

Following initial isolation procedures, approximately 3% of bacterial colonies either failed to proliferate during subsequent subculturing or were unable to be cultured after storage at –80 °C. Consequently, these colonies were excluded from further analyses. Thus, the final analysis encompassed 948 bacterial colonies. From the 948 endophytic bacterial colonies isolated from the sampled tissues, 386 were randomly selected and categorized based on morphological features and biochemical tests. Subsequently, from these grouped colonies, 148 endophytes—representing each morphological group—were randomly chosen and purified for subsequent DNA extraction. This study aims to examine the bacterial population and its temporal variations in the root, stem, leaf, bulk soil, and rhizosphere across healthy plants and those undergoing senescence and death. Statistical analysis using analysis of variance (ANOVA) on 600 samples revealed significant differences in the number of bacterial isolates recovered, both by sample type ($F = 10.42$, $P < 0.05$) and by disease index ($F = 8.99$, $P < 0.05$). Notably, a significantly greater proportion (83.78%) of symptomatic tissues from severely diseased trees (Disease Index = 5) yielded bacterial growth, compared with tissues from trees with lower disease indices, where only 14% of healthy tree samples (DI = 1 and DI = 2) yielded bacterial isolation. Additionally, the bacterial recovery rates from bulk soil and rhizosphere samples were significantly higher than those from root, leaf, and stem tissues ($p < 0.01$), with root samples yielding intermediate recovery rates (Figure 1).

A total of 148 bacterial isolates were identified through 16S rRNA sequencing and biochemical characterization (Table 1) and were classified into 31 bacterial species. However, there was notable variation in the frequency of occurrence of these taxa. Generally, a few species dominated the collection (≥50 isolates throughout the study), namely Stenotrophomonas maltophilia, Pantoea agglomerans, Campylobacter jejuni, Achromobacter xylosoxidans, Serratia marcescens, and Brenneria roseae, while many other species were rare or represented by single isolates (Table 1). The primary bacterial families identified in oak samples included *Alcaligenaceae*, *Bacillaceae*, *Brevibacteriaceae*, *Campylobacteraceae*, *Clostridiaceae*, *Microbacteriaceae*, *Enterobacteriaceae*, *Moraxellaceae*, *Paenibacillaceae*, *Pseudomonadaceae*, *Pectobacteriaceae*, and *Xanthomonadaceae*. In terms of relative abundance, most isolates belonged to the Bacillaceae family (24.32% of the total isolates), followed by Enterobacteriaceae (21.62%) and Xanthomonadaceae (10.13%). Isolates belonging to the Brevibacteriaceae family comprised only 1.35% of the total, with just two isolates identified as members of the genus Brevibacterium (Table 1, Figure 2).

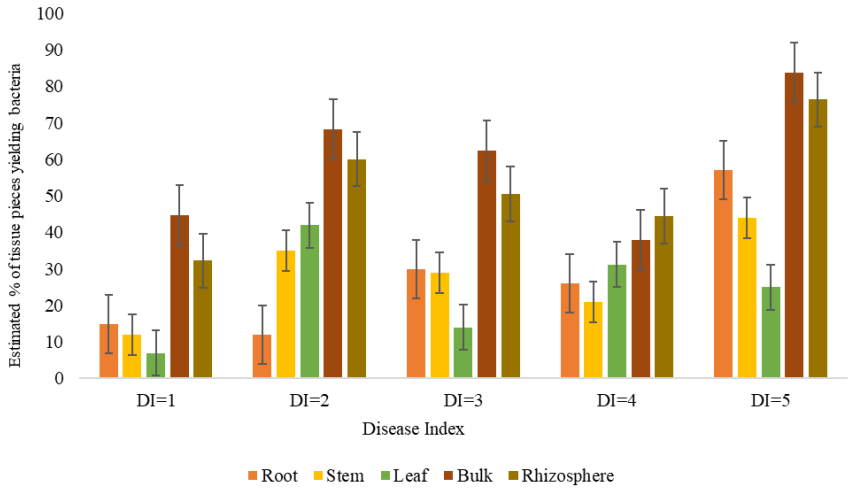

Figure 1. Estimated Bacterial Yield (% Sample Pieces Yielding Bacteria) of Different Sample Types in Healthy and Diseased Quercus Brantii Trees

Table 1. Species of Bacteria Isolated from Different Samples of the Five-disease Index in Eight Sites

Species (Family)	Codes isolate***	Number of isolates in disease index's					Number of isolates in different sample*					Number of isolates in different sites**							
		1	2	3	4	5	Le	Ro	St	Rh	Bu	G	A	E	S	C	O	T	M
Achromobacter Xylosoxidans (Alcaligenaceae)	AcXy	0	5	6	0	0	0	3	0	5	3	6	5	0	0	0	0	0	0
Acinentobacter Calcoacelticus (Moraxellaceae)	AcCa	8	0	0	0	0	2	5	0	1	0	0	5	2	0	1	0	0	0
Bacillus Cereus (Bacillaceae)	BaCe	1	3	0	0	0	2	0	2	0	0	2	1	0	0	1	0	0	0
Bacillus Endophyticus (Bacillaceae)	BaEn	0	1	0	0	0	0	1	0	0	0	0	1	0	0	0	0	0	0
Bacillus Megaterium (Bacillaceae)	BaMe	0	0	0	0	1	0	1	0	0	0	0	1	0	0	0	0	0	0
Bacillus Methylotrophicus (Bacillaceae)	BaMet	1	1	0	0	0	0	0	0	0	2	1	1	0	0	0	0	0	0
Bacillus Mojavensis (Bacillaceae)	BaMo	0	0	3	0	0	2	0	1	0	0	1	1	0	0	1	0	0	0
Bacillus Mycoides (Bacillaceae)	BaMy	0	1	0	0	0	0	0	1	0	0	0	1	0	0	0	0	0	0
Bacillus Pumilus (Bacillaceae)	BaPu	0	0	0	2	3	1	2	2	0	0	0	0	0	0	0	1	2	2
Bacillus Safensis (Bacillaceae)	BaSa	0	2	0	0	0	1	1	0	0	0	1	0	0	0	1	0	0	0
Bacillus Simplex (Bacillaceae)	BaSi	1	2	0	0	0	0	0	3	0	0	1	0	1	0	1	0	0	0
Bacillus Subtilis (Bacillaceae)	BaSu	2	2	0	0	0	1	1	2	0	0	2	0	1	0	1	0	0	0
Bacillus Thuringiensis (Bacillaceae)	BaTh	0	0	1	0	0	1	0	0	0	0	0	0	1	0	0	0	0	0
Bacillus Toyonensis (Bacillaceae)	BaTo	0	1	0	0	0	0	0	1	0	0	0	0	0	1	0	0	0	0
Bacillus Vallismortis (Bacillaceae)	BaVa	1	0	1	0	0	1	0	1	0	0	0	1	0	1	0	0	0	0
Bacillus Velezensis (Bacillaceae)	BaVe	1	1	0	0	0	1	0	1	0	0	0	1	0	1	0	0	0	0
Brenneria goodwinii (Pectobacteriaceae)	BrGo	0	0	0	6	0	2	0	4	0	0	0	0	4	0	0	0	2	0
Brevibacillus Invocate (Paenibacillaceae)	BrIn	0	1	2	0	0	0	0	0	2	1	0	0	2	1	0	0	0	0
Brevibacterium Frigoritolerans (Brevibacteriaceae)	BrFr	0	0	1	0	0	0	0	0	1	0	0	0	0	1	0	0	0	0
Brevibacterium Halotolerans (Brevibacteriaceae)	BrHa	0	0	0	1	0	0	0	0	1	0	0	0	0	1	0	0	0	0
Campylobacter Jejuni (Campylobacteraceae)	CaJe	3	0	4	5	0	0	4	3	5	0	7	0	3	0	0	0	0	2
Clostridium Sp (Clostridiaceae)	ClSP	2	0	3	3	0	2	1	0	0	5	5	2	0	0	0	0	1	0
Dickeya Chrysanthemi (Enterobacteriaceae)	DiCh	0	1	0	3	5	1	2	4	0	2	0	0	3	0	2	3	1	0
Lysinibacillus Fusiformis (Bacillaceae)	LyFu	1	1	0	0	0	1	1	0	0	0	0	0	0	0	2	0	0	0
Lysinibacillus Xylanilyticus (Bacillaceae)	LyXy	0	0	2	0	0	1	1	0	0	0	0	2	0	0	0	0	0	0
Microbacterium Aurantiacum (Microbacteriaceae)	MiAu	0	3	2	0	0	1	0	1	1	2	2	0	0	0	3	0	0	0
Paenibacillus Apiarius (Paenibacillaceae)	PaAp	2	1	0	0	0	0	1	2	0	0	0	0	0	0	0	0	0	3
Pantoea Agglomerans (Enterobacteriaceae)	PaAg	0	0	5	0	9	0	4	6	0	4	0	0	0	4	0	5	0	5

Table 1. Continued.

Species (Family)	Codes isolate***	Number of isolates in disease index's					Number of isolates in different sample*					Number of isolates in different sites**							
		1	2	3	4	5	Le	Ro	St	Rh	Bu	G	A	E	S	C	O	T	M
Pseudomonas Granadensis (Pseudomonadaceae)	PsGr	0	0	3	3	1	0	0	0	3	4	0	0	0	0	0	0	0	7
Serratia Marecescence (Enterobacteriaceae)	SeMa	0	0	2	3	4	2	0	0	3	4	0	0	0	3	0	3	3	0
Stenotrophomonas Maltophilia (Xanthomonadaceae)	StMa	0	0	3	5	7	9	6	0	0	0	0	0	0	0	4	2	5	4

*Le: Leaf; Ro: Root; St: Stem; Rh: Rhizosphere, Bu: Bulk**G: Gale jar; A: Arghavan; E: Eyvan; S: Sale abad; C: Chavar; O: Chogha sabz; T: Tange dalab; M: Malek shahi. ***Species codes are first three letters of genus + first three letters of specific epithet

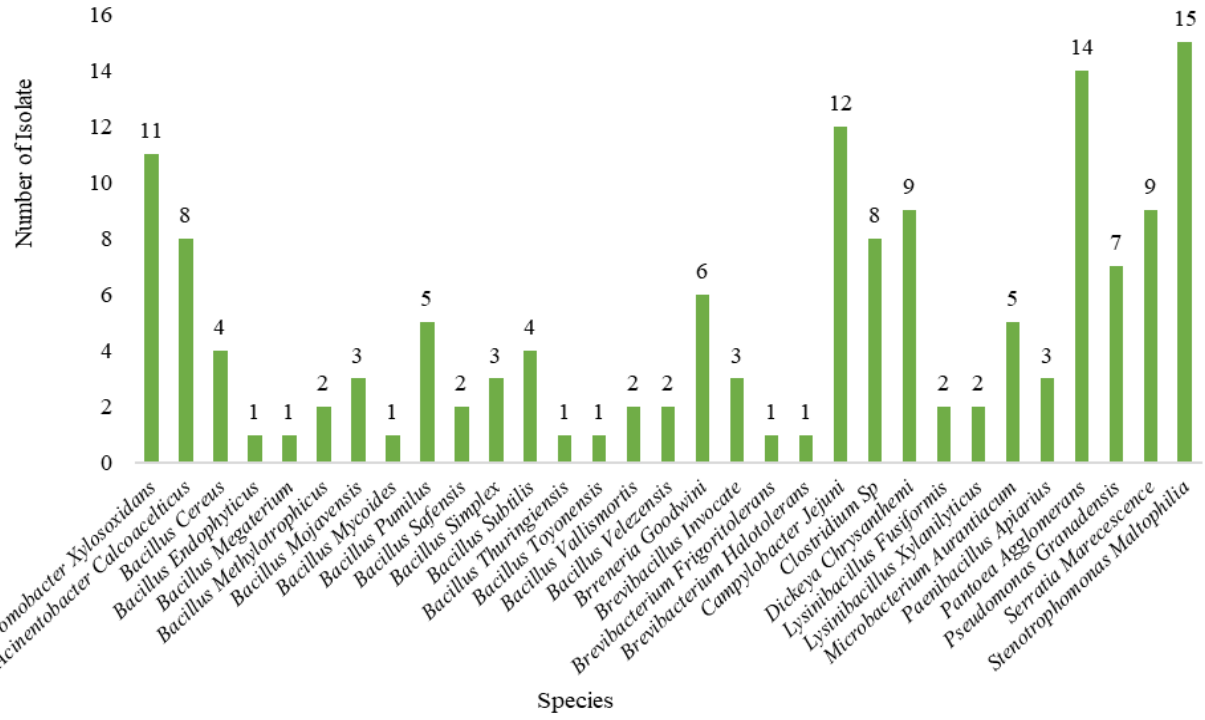

Figure 2. Abundance of Isolates for 31 Species Isolated from Various Samples Types

The composition of bacterial isolates by sampling site is illustrated in Figure 3 based on family-level classifications. Members of the *Bacillaceae* family were detected at all sampled locations. Notable differences in the relative abundances of *Bacillaceae* and *Enterobacteriaceae* families were observed across the eight sites. Specifically, isolates from the Brevibacteriaceae family were recovered only in the Saleh Abad region, while those from the *Pseudomonadaceae* family were exclusive to the Malek Shahi area. Additionally, Bacillaceae isolates in the Arghavan site and *Enterobacteriaceae* isolates in the Chogha Sabz site exhibited distinct distribution patterns compared to isolates from other locations (Figure 3).

The relative composition of the bacterial isolates by disease index, categorized by family, is depicted in Figure 4. The most pronounced variation in bacterial family composition was observed in DI=3, followed by DI=4. Across all disease indices, the *Bacillaceae* family was present. Moraxellaceae isolates were recovered exclusively in DI=1, while *Pectobacteriaceae* were detected only in DI=4. A notable observation is that most Bacillus species were prevalent at lower disease indices, indicating their dominance in the early stages of disease (indices 1 and 2). In contrast, the *Enterobacteriaceae* family predominated in samples from trees at advanced disease stages (indices 4 and 5). The proportion of *Brevibacteriaceae* isolates remained consistent across both DI=3 and DI=4 (Figure 4).

The precise causative agents of oak decline in Iran remain unresolved, consistent with the syndrome's multifactorial nature (Bashiri *et al.*, 2024). Although only a few studies have directly explored bacterial involvement in Persian oak decline, they do implicate cultivable bacteria in affected Zagros stands (Ahmadi *et al.*, 2019; Moradi-Amirabad *et al.*, 2019). Comparable reports from other regions likewise associate bacteria with oak decline syndromes, including early observations of aerobic bacteria on declining oaks in Europe and the subsequent description of taxa now linked to Acute Oak Decline (AOD) in the UK (Denman *et al.*, 2012; Doonan *et al.*, 2019).

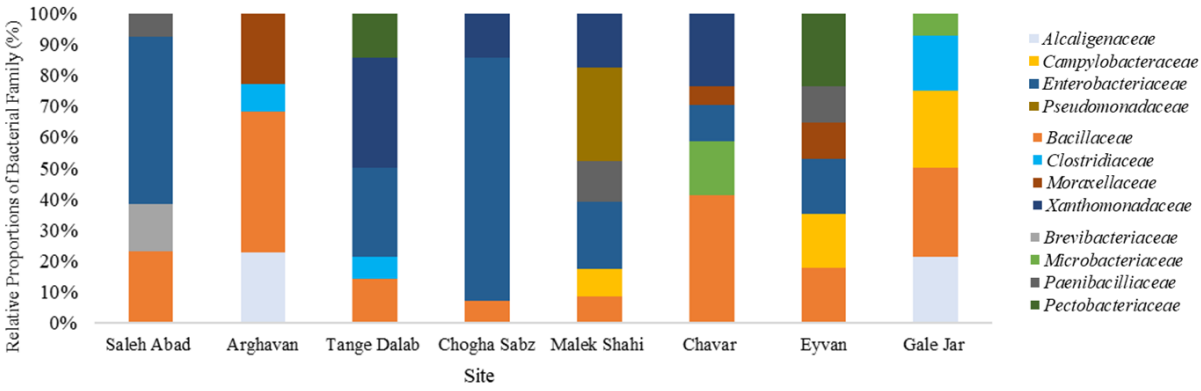

Figure 3. Bacterial Family Distribution of the Culturable Endophytic Isolates Obtained from Eight Sites

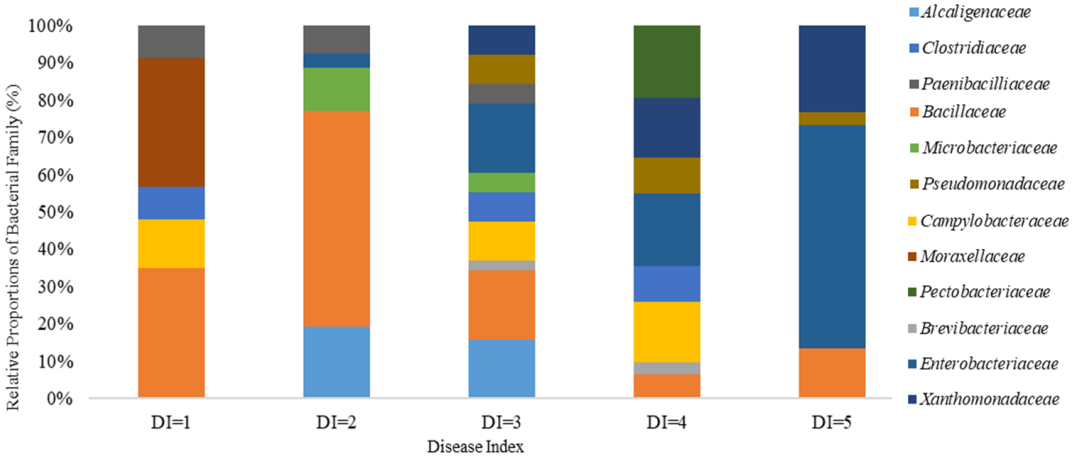

Figure 4. Bacterial Family Distribution of the Culturable Endophytic Isolates Obtained from Five Disease Indices

To address this gap, we profiled the cultivable bacterial communities in symptomatic oak tissues and contrasted them with those from asymptomatic trees, aiming to resolve site-level patterns, disease-stage differences, and sample-type effects while also screening for putative pathogens and potential biocontrol taxa. Such case–control comparisons of healthy versus diseased microbiomes provide a pragmatic filter for prioritizing candidate organisms for follow-up pathogenicity testing.

This investigation clearly revealed strong similarities in the species composition of bacterial communities in symptomatic tissues compared with those in healthy tissues, regardless of the sampling site. Importantly, a culture-dependent approach was deliberately chosen over culture-independent metagenomics, as our study required living microorganisms to assess their potential roles in suppressing oak pathogens. The colonization frequency of endophytic bacteria appeared to be influenced by both disease index and sampling site (Figure 1). The population density of culturable bacteria in DI=5 (advanced disease stage) samples of bulk material was comparable to densities reported from symptomatic tissue fragments of diseased trees by Denman *et al.* (2016). However, bacterial diversity peaked in DI=3 (Figure 4), suggesting that at this intermediate stage of disease, trees may still be metabolically active, hosting a mix of pathogenic and endophytic bacteria (Ou *et al.*, 2019; Berg *et al.*, 2019). Conversely, the sharp reduction in bacterial diversity observed in DI=5 (Figure 4) likely reflects the collapse of tree health, with most endophytes absent and the remaining bacterial community predominantly pathogenic.

Intriguingly, we also isolated a broad suite of non-oak–specialist bacteria from symptomatic tissues. These included *Pantoea agglomerans* and *Pseudomonas granadensis*, both reported from diverse crop and woody hosts and detected in our material in DI = 3 and DI = 5 samples, suggesting that, under conducive conditions, they may also act as pathogens in oak (Geraffi *et al.*, 2023). Among the 148 isolates, 38 were *Bacillus* (including *Paenibacillus* and *Lysinibacillus*) recovered from multiple plant parts (Table 1) and present at all sites, with higher frequencies at Chavar and Arghavan (Figure 3). *Bacillus* spp. predominated in low disease indices (DI = 1–2), whereas *B. megaterium* and *B. pumilus* occurred at DI = 5. Consistent with current understanding, *B. pumilus* has been documented as a tree pathogen, while *B. Megaterium* (≡ *Priestia megaterium*) is generally non-pathogenic and widely recognized for biocontrol/PGPR potential (Zhang *et al.*, 2023). In a broader biogeographic context, Iranian Hyrcanian forest soils show bacterial communities structured primarily by vegetation and edaphic factors, whereas Zagros oak systems under decline exhibit communities more strongly filtered by chronic water stress

and decline-associated bacteria—aligning with the prominence of non-oak specialists and specific lineages at higher DI classes in our dataset (Bayranvand *et al.*, 2021; Mehri *et al.*, 2024).

Intriguingly, we also recovered a broad suite of non-oak–specialist bacteria from symptomatic tissues. These included *Pantoea agglomerans* and *Pseudomonas granadensis*, both reported on diverse crop and woody hosts; in our material, they occurred at DI = 3 and DI = 5, suggesting that under conducive conditions, they may also act as pathogens in oak. Among 148 isolates, 38 were *Bacillus* (including *Paenibacillus* and *Lysinibacillus*), recovered from multiple plant parts (Table 1), and were more frequent at Chavar and Arghavan (Figure 3). *Bacillus* spp. predominated in low DI (1–2), whereas *B. megaterium* and *B. pumilus* were detected at DI = 5. Notably, *B. pumilus* is documented as a tree pathogen, while *B. Megaterium* (≡ *Priestia megaterium*) is generally non-pathogenic and widely recognized for biocontrol/PGPR potential; the ubiquity and protective roles of *Bacillus* may partly explain the absence of visible symptoms at certain sites (Mazlan *et al.*, 2019; Lahlali *et al.*, 2022; Geraffi *et al.*, 2023; Zhang *et al.*, 2023; Cea-Torrescassana *et al.*, 2024). Complementing our findings, studies from Iranian forest soils—particularly the Hyrcanian broadleaf forests—show that soil bacterial community composition tracks vegetation and edaphic context, with soil chemistry and plant mycorrhizal type emerging as dominant drivers along altitudinal and habitat gradients (Bayranvand *et al.*, 2021). In contrast, Zagros oak systems experiencing decline exhibit communities that are more strongly filtered by chronic water stress and decline-associated pathogens, with symptomatic tissues repeatedly yielding taxa linked to lesion formation (e.g., *Brenneria goodwinii*, *Stenotrophomonas maltophilia*) and shifts consistent with a stress-enabled disease complex (Ahmadi *et al.*, 2019; Mehri *et al.*, 2024). Taken together, whereas Hyrcanian soils largely reflect vegetation–soil controls under humid temperate conditions, the Zagros oak microbiome reflects a pathogen–stress signature under semi-arid pressure, aligning with our observation that non-oak specialists and specific bacterial lineages become prominent in high DI classes.

Interestingly, the majority of isolates from early disease stages (DI=1 and DI=2) were Gram-positive bacteria, which often play beneficial roles in plant systems. The characteristics of bacteria isolated from healthy samples suggest that these communities are dominated by plant-associated and ubiquitous species. Notably, *Clostridium spp*. and *Acinetobacter calcoaceticus*, recovered from healthy samples, are recognized as plant growth-promoting rhizobacteria (PGPR) capable of suppressing potentially harmful microorganisms (Rokhbakhsh-Zamin *et al.*, 2011). *Campylobacter jejuni*, isolated from samples from DI=1, 3, and 4, is a Gram-negative, spiral-shaped bacterium primarily known as a pathogen in humans, animals, and, occasionally, plants (CDC, 2014). Given that *Campylobacter* species are frequently isolated from fruits and vegetables consumed raw (Brandl *et al.*, 2004), their association with both symptomatic and asymptomatic oak tissues is intriguing. *Achromobacter xylosoxidans*, formerly *Alcaligenes xylosoxidans*, a motile Gram-negative rod known since 1971 (De Baets *et al.*, 2007), was also recovered from various health statuses in oak tissues. While this bacterium is recognized as an environmental opportunistic human pathogen (Jakobsen *et al.*, 2013), it has also been reported as a biocontrol agent and PGPR (Abdel-Rahman *et al.*, 2014) and has potential for phytoremediation (Ho *et al.*, 2013). Recent studies have further explored the potential of *Achromobacter xylosoxidans* in enhancing plant resistance to pathogens, highlighting its biocontrol potential in forest ecosystems (Ranjbar *et al.*, 2024).

3.2. Distribution patterns of plants and soil microbiotas

3.2.1. Ordination of endophytic Bacteria communities

We conducted a permutational multivariate analysis of variance (PERMANOVA) using a Bray-Curtis distance matrix and 999 permutations to assess how bacterial communities were influenced by three factors. The PERMANOVA results revealed a significant impact of the sampling site on the composition of bacterial assemblages (p-value = 0.001, F-value = 4.4769). Additionally, bacterial communities were found to be significantly affected by the disease index (p-value = 0.001, F = 5.1034). However, no significant differences were observed among the different sample types (p-value = 0.24, F = 1.29).

In the two-dimensional MDS plot (Figure 5), the composition of bacterial species was notably distinct in samples from the Tange Dalab and Gale Jar sites when compared to the other locations. Among them, the Tange Dalab site showed the closest resemblance in bacterial species composition to that of the Chogha Sabz site. However, high variability in bacterial composition was observed across samples from Chavar, Malek Shahi, Eyvan, and Arghavan (Figure 5a).

When considering variation between samples from different disease indices (DIs), as shown in Figure 5b, DI 5 and DI 1 displayed the greatest differences from the other disease indices.

Table 2. Statistical Testing of Bacterial Community Composition in Response to Different Environmental Variables

Variation/index	Bacterial community composition			
	Sum of Sqs	R^2	F-value	P
Site	0.0173	0.269	4.4769	0.001***
Disease index	0.0034	0.053	5.103	0.001***
Sample type	0.0035	0.055	1.373	0.177 ^{ns}
Site× Disease index	0.0064	0.1007	1.675	0.033*
Sample type × Disease index	0.0029	0.0459	1.090	0.395 ^{ns}
Sample type × Site	0.0180	0.280	1.246	0.133^{ns}

Mean significant in different probability level: Signif. codes: 0 '***'; 0.001 '**'; 0.01 '*'; ns: not significant.

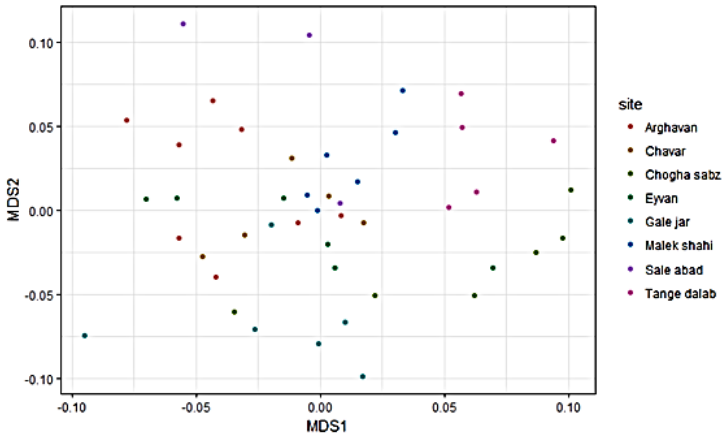

(a)

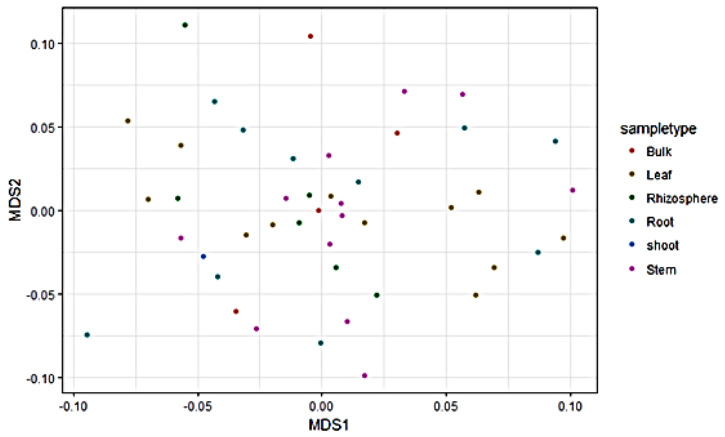

(b)

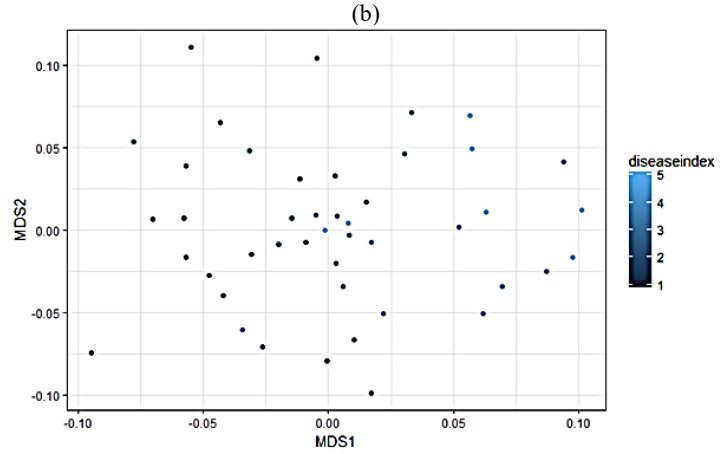

(c)

Figure 5. Nonmetric Multidimensional Scaling (NMDS) Plot Showing Bacteria Species Composition Similarity Among (A) Plots Under Different Sites, (B) Different Sample Types, and (C) Different Disease Indexes

Using canonical correspondence analysis (CCA), we identified and plotted the most significant ecological variables correlated with changes in bacterial community composition (Figure 6). This ordination clearly shows how bacterial taxa and individual sample points are distributed along the main environmental gradients, with vectors representing ecological variables such as sampling site, disease index, and sample type. The direction and length of these vectors indicate both the strength and the nature of their correlation with the canonical axes: samples and taxa positioned in the same direction as a given vector are positively associated with that variable, whereas those located in the opposite direction show a negative or weaker association. In particular, the analysis revealed distinct clustering of samples according to site and disease index, demonstrating that bacterial communities from different locations or health conditions occupy separate regions in the CCA ordination space. This pattern indicates that environmental variables, especially sampling site, followed by disease index and sample type, exert a substantial influence on the structure of the bacterial communities, supporting the view that local ecological conditions are key drivers of endophytic bacterial community composition (Figure 6).

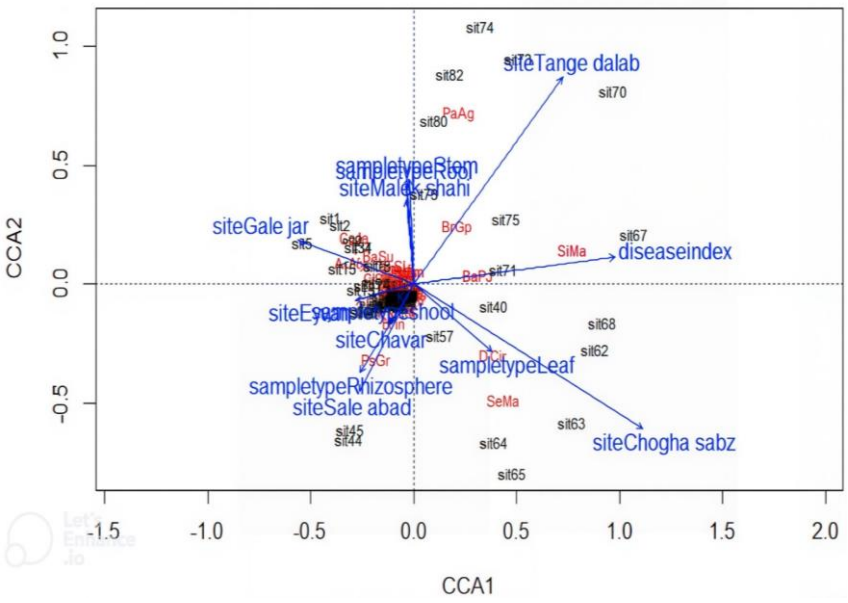

Figure 6. Canonical Correspondence Analysis (CCA) Plotting Ecological Variables Correlated with Variation in Bacterial Taxa and Sample Points

The CCA biplot illustrates the influence of environmental parameters using arrows, with the length of each arrow representing its relative importance (Liu *et al.*, 2009). Notably, the Tange Dalab and Chogha Sabz sites displayed the longest arrows, highlighting their substantial impact on shaping the bacterial community. The disease index also showed a significant correlation with bacterial taxa variance in the CCA. The first axis (CCA1) accounted for 27.43% of the total variation, driven mainly by contributions from Chogha Sabz, Eyvan, and Gale Jar sites, as well as the disease index. The second axis (CCA2) explained 16.29% of the variation, predominantly influenced by the Malek Shahi, Chavar, Tange Dalab, and Saleh Abad sites, as well as by the different sample types (stem, root, and rhizosphere). In the analysis, CCA1 revealed that the disease index contributed approximately 14.95% to the variation in bacterial taxa distribution, while the Tange Dalab site contributed around 11.44%. Additionally, the majority of species in the CCA plot were located near the center of the axes, indicating a weak association between these taxa and the measured environmental factors. The ordination diagram further highlighted a strong association of *Brenneria goodwinii* and *Pantoea agglomerans* with the Tange Dalab site. CCA analysis also revealed significant correlations between *Brenneria roseae* (DiCh) and *Serratia marcescens* (SeMa) with the Chogha Sabz site and the leaf sample type (r=0.5 and r=0.42, respectively). Similarly, *Pseudomonas granadensis* (PsGr) showed a significant correlation with the Saleh Abad site and the rhizosphere sample type (r=0.45, P=0.04). *Bacillus pumilus* (BaPu) and *Stenotrophomonas maltophilia* (StMa) were also significantly associated with the disease index (r=0.45 and r=0.47, P=0.04).

The results from the ordination analysis demonstrated that endophytic bacterial communities differed significantly on a landscape scale—that is, across different sites—but not among sample types (Figure 5, Table 2). Specifically, the composition of bacterial species at the Tange Dalab and Gale Jar sites was highly distinct from that at other sites, with Tange Dalab's bacterial composition most closely resembling that of Chogha Sabz (Figure 5a). Literature review and field observations suggest that bacteria associated with trees at these sites are often pathogenic, particularly members of the Enterobacteriaceae and Xanthomonadaceae families. Moreover, field observations confirmed that Tange Dalab and Chogha Sabz were focal points of contamination. PERMANOVA analysis showed no significant differences among sample types (Table 2), and Figure 5b shows that points representing the sample types were intermixed on the plot, indicating no clear differences in bacterial species composition among the sample types. However, among sample types, the highest diversity of identified bacterial isolates was observed in root and stem samples (Table 1).

It is known that some bacteria colonizing the rhizoplane can penetrate plant roots and migrate to stems and leaves, although bacterial density generally decreases from roots to aerial organs (Compant *et al.*, 2010). Sturz *et al.* (1997) similarly reported that 87% of endophytic bacteria in the lower foliage of red clover originated from inside roots and root nodules. The relatively low diversity of endophytic bacteria in leaves and stems could be attributed to the harsher conditions of the phyllosphere, including exposure to UV radiation, desiccation, reactive oxygen species, and limited nutrient availability (Lindow & Brandl, 2003). Recent studies have further emphasized the importance of endophytes in enhancing plant resilience to environmental stressors, particularly in forest ecosystems, where endophytic bacteria are thought to play crucial roles in mitigating abiotic stress. In oak ecosystems, for instance, the presence of specific bacterial species, such as *Achromobacter xylosoxidans* and *Bacillus* spp., has been linked to enhanced resistance to pathogens and environmental stress (Mehri *et al.*, 2024; Jamali *et al.*, 2024).

Additionally, advances in microbiome analysis techniques, such as metagenomics, have revealed more

complex interactions between endophytic communities and their plant hosts, shedding light on the ecological roles of these microorganisms in maintaining forest health (Mirhashemi *et al.*, 2022).

A logical hypothesis is that the plant's life span—whether annual or perennial—might also influence the diversity and composition of endophytic bacteria, especially in leaves, given that most endophytes are soil-derived and migrate from roots to other tissues. In our study of the perennial oak species *Quercus brantii*, which seasonally sheds its leaves in temperate climates, we found clear evidence of higher endophytic bacterial diversity in roots and distinct bacterial communities among leaf, stem, and root samples.

Our results also revealed striking similarities in bacterial species composition between cultivable lesion microbiomes from diseased and healthy trees (across disease indices), irrespective of site (Table 2 and Figure 5c). This pattern has been observed in several previous studies (Denman *et al.*, 2016). The overall health status of trees (DI=1 and DI=2) had only a minimal effect on the general oak microbiome, indicating that there was no consistent shift toward a disease-associated bacterial community across sites. Instead, symptomatic tissues (DI=3, 4, and 5) displayed only small, site-masked global changes.

This observation is reinforced by the finding that distinct site-specific shifts were observed in oak-associated communities in symptomatic tissues, particularly at advanced disease stages when the influence of other sites was excluded. This suggests that observed community changes are closely tied to geographic conditions, emphasizing the role of spatial structuring even in the context of the Acute Oak Decline syndrome (Denman *et al.*, 2014; Mehri *et al.*, 2024).

Additionally, our study highlights the complexity of bacterial community shifts in response to abiotic stressors and pathogen interactions, particularly in oak ecosystems where environmental factors exacerbate disease progression (Jamali *et al.*, 2024). To investigate the relationships between bacterial community composition and environmental variables, we analyzed different bacterial taxa using CCA (Figure 6).

The results showed that the sampling site had a clear effect on bacterial communities, with *Brenneria roseae* and *Serratia marcescens* associated with Chogha Sabz, and *Pseudomonas granadensis* correlated with Saleh Abad. This indicates that geographical distance plays a major role in shaping the oak microbiome, pointing to strong spatial structuring and local environmental adaptation, as previously demonstrated in Tamarix and oak trees (Denman *et al.*, 2016).

These findings suggest that the sampling zone is a more influential factor than sample type in determining the structure of the endophytic bacterial community in *Q. brantii*. This observation is consistent with the stark differences between habitats in terms of exposure (to air, sun, wind, rain, moisture, and aeration) and nutrient availability (Andreote *et al.*, 2014). On the other hand, specific soil properties, such as pH at each site, are also likely to influence microbial community composition (Drenovsky *et al.*, 2004).

Fierer and Jackson (2006) demonstrated that pH impacts the diversity and composition of microbial communities in various terrestrial and aquatic environments. Additionally, salinity has been shown to affect bacterial composition and diversity across diverse habitats (Wakelin *et al.*, 2012). Therefore, it can be concluded that the sampling site plays a more critical role in shaping the endophytic bacterial community of *Q. brantii*, as illustrated in Figures 5a and 6.

4. Conclusion

This study reveals the diverse community of endophytic bacteria in Persian oak *(Quercus brantii*), shaped by both site and tissue type. It provides the first insights into bacterial microbiomes of healthy and diseased native oaks in Iran and establishes a culture collection for future research. A clear shift in cultivable bacteria was observed between healthy and diseased trees, with the latter harboring three distinct species—suggesting oak decline is likely due to polymicrobial infection rather than a single pathogen. Expanding the study to include larger samples and European sites with similar symptoms could uncover broader patterns. Further research is needed to understand the ecological roles of these microbes, including their interactions with insects, with one another, and with the host plant.

Conflict of interest

The authors declare no conflict of interest.

Acknowledgment

The authors are very grateful to Ebrahim Karimi, Saadi Karami, and Amin Alidadi for their kind technical assistances in development of the protocols.

Ethical approval

This article does not contain any studies with human participants or animals performed by any of the authors.

Funding

None declared.

Authors' Contributions

All authors have read and approved the final version of the manuscript.

References

Abdel-Rahman, H. M., Salem, A. A., Moustafa, M. M., & El-Garhy, H. A. (2017). A novice Achromobacter sp. EMCC1936 strain acts as a plant-growth-promoting agent. Acta physiologiae plantarum, 39, 1-15. https://doi.org/10.0.3.239/s11738-017-2360-6.

Ahmadi, E., Kowsari, M., Azadfar, D., & Salehi Jouzani, G. (2019). *Bacillus pumilus* and *Stenotrophomonas maltophilia* as two potentially causative agents involved in Per-sian oak decline in Zagros forests (Iran). Forest Pathology, 49(5), e12541. https://doi.org/10.1111/efp.12541.

Ahmadi, R., Kiadaliri, H., Mataji, A., & Kafaki, S. (2014). Oak forest decline zonation using AHP model and GIS technique in Zagros forests of Ilam province. J Biodivers Environ Sci, 4(3), 141-50.

Alidadi, A., Javan-Nikkhah, M., Kowsari, M., Karami, S., & Rastaghi, M. E. (2018). Some species of fungi associated with declined Persian oak trees in Ilam province with emphasis on new records to mycobiota of Iran. *Rostaniha,* 19(2), 75–91. https://doi.org/10.22092/botany.2019.122177.1105

Amaral-Zettler, L. A., Zettler, E. R., Theroux, S. M., Palacios, C., Aguilera, A., & Am-ils, R. (2011). Microbial community structure across the tree of life in the extreme Rio Tinto. The ISME journal, 5(1), 42-50. https://doi.org/10.1038/ismej.2010.101.

Andreote, F. D., Gumiere, T., & Durrer, A. (2014). Exploring interactions of plant mi-crobiomes. Scientia agrícola, 71, 528-539. https://doi.org/10.1590/0103-9016-2014-0195.

Azimi, P., Safaie, N., Zamani, S. M., Mojerlou, S., & Alizadeh, M. (2023). Climate-induced vegetation dynamics associated with the prevalence of charcoal oak disease in Zagros forests. Industrial Crops and Products, 200, 116885. https://doi.org/10.1016/j.indcrop.2023.116885

BakhshiGanje, M., Mahmoodi, S., Ahmadi, K., & Mirabolfathy, M. (2024). Potential distribution of *Biscogniauxia mediterranea* and *Obolarina persica* causal agents of oak charcoal disease in Iran's Zagros forests. Scientific Reports, 14(1), 7784. https://doi.org/10.1038/s41598-024-57298-2.

Bashiri, S., & Abdollahzadeh, J. (2024). Taxonomy and pathogenicity of fungi associated with oak decline in northern and central Zagros forests of Iran with emphasis on coelomycetous species. *Frontiers in Plant Science*, 15, 1377441. https://doi.org/10.3389/fpls.2024.1377441.

Bayranvand, M., Akbarinia, M., Salehi Jouzani, G., Gharechahi, J., Kooch, Y., & Baldrian, P. (2021). Composition of soil bacterial and fungal communities in relation to vegetation composition and soil characteristics along an altitudinal gradient. *FEMS microbiology ecology*, *97*(1), fiaa201.

Berg, J. J., Harpak, A., Sinnott-Armstrong, N., Joergensen, A. M., Mostafavi, H., Field, Y., ... & Coop, G. (2019). Reduced signal for polygenic adaptation of height in UK Bi-obank. *Elife*, 8, e39725. https://doi.org/10.7554/eLife.39725.

Bergey, D. H., & Breed, R. S. (1948). Manual of determinative bacteriology. Williams & Wilkins Company.

Biosca, E. G., González, R., López-López, M. J., Soria, S., Montón, C., Pérez-Laorga, E., & López, M. M. (2003). Isolation and characterization of *Brenneria quercina*, causal agent for bark canker and drippy nut of Quercus spp. in Spain. *Phytopathology*, 93(4), 485-492. https://doi.org/10.1094/PHYTO.2003.93.4.485.

Brady, C. L., Cleenwerck, I., Denman, S., Venter, S. N., Rodríguez-Palenzuela, P., Coutinho, T. A., & De Vos, P. (2012). Proposal to reclassify Brenneria quercina (Hil-debrand and Schroth 1967) Hauben *et al.* 1999 into a new genus, *Lonsdalea* gen. nov., as *Lonsdalea quercina* comb. nov., descriptions of *Lonsdalea quercina* subsp. *quercina* comb. nov., *Lonsdalea quercina* subsp. *iberica* subsp. nov. and *Lonsdalea quercina* subsp. *britannica* subsp. nov., emendation of the description of the genus *Brenneria*, re-classification of *Dickeya dieffenbachiae* as *Dickeya dadantii* subsp. *dieffenbachiae* comb. nov., and emendation of the description of *Dickeya dadantii*. *International Journal of Systematic and Evolutionary Microbiology*, 62(Pt_7), 1592-1602. https://doi.org/10.1099/ijs.0.035055-0

Brady, C., Hunter, G., Kirk, S., Arnold, D., & Denman, S. Brady, C., Hunter, G., Kirk, S., Arnold, D., & Denman, S. (2014). *Rahnella victoriana* sp. nov., *Rahnella bruchi* sp. nov., *Rahnella woolbedingensis* sp. nov., classification of *Rahnella* genomospecies 2 and 3 as *Rahnella variigena* sp. nov. and *Rahnella inusitata* sp. nov., respectively and emended description of the genus *Rahnella*. Systematic and applied microbiology, 37(8), 545-552. https://doi.org/10.1016/j.syapm.2014.09.001.

Brandl, M. T., Haxo, A. F., Bates, A. H., & Mandrell, R. E. (2004). Comparison of Survival of *Campylobacter jejuni* in the Phyllosphere with That in the Rhizosphere of Spinach and Radish Plants. *Applied and Environmental Microbiology*, 70(2), 1182-1189. https://doi.org/10.1128/AEM.70.2.1182-1189.2004.

Compant, S., Van Der Heijden, M. G., & Sessitsch, A. (2010). Climate change effects on beneficial plant–microorganism interactions. F*EMS microbiology ecology*, 73(2), 197-214. https://doi.org/10.1111/j.1574-6941.2010.00900.x.

Constantin, M., Negut, C. D., Barna, C., Cîmpeanu, C., & Ardelean, I. I. (2016). Isolation and identification of soil bacteria able to efficiently remove copper from culture mediums. Rom J Phys, 61, 707-717.

De Baets, F., Schelstraete, P., Van Daele, S., Haerynck, F., & Vaneechoutte, M. (2007). *Achromobacter xylosoxidans* in cystic fibrosis: prevalence and clinical rele-vance. Journal of Cystic Fibrosis, 6(1), 75-78. https://doi.org/10.1016/j.jcf.2006.05.011.

Denman, S., & Webber, J. (2009). Oak declines: new definitions and new episodes in Britain. https://doi.org/10.1093/forestry/cpp033.

Denman, S., Brown, N., Kirk, S., Jeger, M., & Webber, J. (2014). A description of the symptoms of Acute Oak Decline in Britain and a comparative review on causes of similar disorders on oak in Europe. Forestry: An International Journal of Forest Re-search, 87(4), 535-551.https://doi.org/10.1093/forestry/cpu010.

Denman, S., Doonan, J., Ransom-Jones, E., Broberg, M., Plummer, S., Kirk, S., ... & McDonald, J. E. (2018). Microbiome and infectivity studies reveal complex polyspe-cies tree disease in Acute Oak Decline. The ISME journal, 12(2), 386-399. https://doi.org/10.1038/ismej.2017.170.

Denman, S., Plummer, S., Kirk, S., Peace, A., & McDonald, J. E. (2016). Isolation stud-ies reveal a shift in the cultivable microbiome of oak affected with Acute Oak De-cline. *Systematic and Applied Microbiology*, 39(7), 484-490. https://doi.org/10.1016/j.syapm.2016.07.002.

Doonan, J., Denman, S., Pachebat, J. A., & McDonald, J. E. (2019). Genomic analysis of bacteria in the Acute Oak Decline pathobiome. *Microbial genomics*, *5*(1), e000240. https://doi.org/10.1099/mgen.0.000240.

Drenovsky, R. E., Vo, D., Graham, K. J., & Scow, K. M. (2004). Soil water content and organic carbon availability are major determinants of soil microbial community com-position. Microbial ecology, 48, 424-430.https://doi.org/10.1007/s00248-003-1063-2.

Embarcadero-Jiménez, S., Rivera-Orduña, F. N., & Wang, E. T. (2016). Bacterial communities estimated by pyrosequencing in the soils of chinampa, a traditional sus-tainable agro-ecosystem in Mexico. *Journal of soils and sediments*, 16, 1001-1011. https://doi.org/10.1007/s11368-015-1277-1.

Fierer, N., & Jackson, R. B. (2006). The diversity and biogeography of soil bacterial communities. *Proceedings of the National Academy of Sciences,* 103(3), 626-631.https://doi.org/10.1073/pnas.0507535103.

Geraffi, N., Gupta, P., Wagner, N., Barash, I., Pupko, T., & Sessa, G. (2023). Comparative sequence analysis of pPATH pathogenicity plasmids in *Pantoea agglomerans* gall-forming bacteria. *Frontiers in Plant Science*, *14*, 1198160. https://doi.org/10.3389/fpls.2023.1198160.

Gosling, R. H., Jackson, R. W., Elliot, M., & Nichols, C. P. (2024). Oak declines: Reviewing the evidence for causes, management implications and research gaps. *Ecological Solutions and Evidence*, 5(4), e12395.https://doi.org/10.1002/2688-8319.12395.

Hall, R. I., & Smol, J. P. (1992). A weighted—averaging regression and calibration model for inferring total phosphorus concentration from diatoms in British Columbia (Canada) lakes. Freshwater Biology, 27(3), 417-434.https://doi.org/10.1111/j.1365-2427.1992.tb00551.x.

Ho, Y. N., Hsieh, J. L., & Huang, C. C. (2013). Construction of a plant–microbe phy-toremediation system: Combination of vetiver grass with a functional endophytic bac-terium, *Achromobacter xylosoxidans* F3B, for aromatic pollutants remov-al. Bioresource Technology, 145, 43-47. https://doi.org/10.1016/j.biortech.2013.02.051.

Inácio, M. L., Henriques, J., Guerra-Guimaraes, L., Gil Azinheira, H., Lima, A., & Sou-sa, E. (2011). *Platypus cylindrus* Fab.(Coleoptera: Platypodidae) transports Biscog-niauxia mediterranea, agent of cork oak charcoal canker. Bol. San. Veg. Plagas, 37, 181-186.

Ishihara, M., Takikawa, Y., Akiba, M., & Kawabe, Y. (2015). A new bacterial disease observed on *Q uercus myrsinifolia*. *Forest Pathology*, 45(6), 459-466. https://doi.org/10.1111/efp.12195.

Jakobsen, T. H., Hansen, M. A., Jensen, P. Ø., Hansen, L., Riber, L., Cockburn, A., ... & Bjarnsholt, T. (2013). Complete Genome Sequence of the Cystic Fibrosis Pathogen *Achromobacter xylosoxidans* NH44784-1996 Complies with Important Pathogenic Phenotypes. PloS one, 8(7), e68484. https://doi.org/10.1371/journal.pone.0068484.

Jamali, S., & Haack, R. A. (2024). From Glory to Decline: Uncovering Causes of Oak Decline in Iran. Forest Pathology, 54(5), e12898. https://doi.org/10.1111/efp.12898.

Jin, H., Yang, X. Y., Yan, Z. Q., Liu, Q., Li, X. Z., Chen, J. X., ... & Qin, B. (2014). Characterization of rhizosphere and endophytic bacterial communities from leaves, stems and roots of *medicinal Stellera chamaejasme L.* Systematic and Applied Micro-biology, 37(5), 376-385. https://doi.org/10.1016/j.syapm.2014.05.001.

Li, Y., He, W., Ren, F., Guo, L., Chang, J., Cleenwerck, I., ... & Wang, H. (2014). A canker disease of *Populus*× *euramericana* in China caused by *Lonsdalea quercina subsp. populi. Plant Disease*, 98(3), 368-378. https://doi.org/10.1094/PDIS-01-13-0115-RE

Linaldeddu, B. T., Sirca, C., Spano, D., & Franceschini, A. (2009). Physiological re-sponses of cork oak and holm oak to infection by fungal pathogens involved in oak de-cline. Forest Pathology, 39(4), 232-238. https://doi.org/10.1111/j.1439-0329.2008.00579.x.

Lindow, S. E., & Brandl, M. T. (2003). Microbiology of the phyllosphere. *Applied and environmental microbiology*, 69(4), 1875-1883. https://doi.org/10.1128/AEM.69.4.1875-1883.2003.

Mehri, S., Alesheikh, A. A., & Lotfata, A. (2024). Abiotic factors impact on oak forest decline in Lorestan Province, Western Iran. Scientific reports, 14(1), 3973.https://doi.org/10.1038/s41598-024-54551-6.

Minchin, P. R. (1987). Simulation of multidimensional community patterns: towards a comprehensive model. Vegetatio, 71, 145-156. https://doi.org/10.1007/BF00039167.

Mirhashemi, H., Heydari, M., Karami, O., Ahmadi, K., & Mosavi, A. (2023). Modeling climate change effects on the distribution of oak forests with machine learning. Forests, 14(3), 469. https://doi.org/10.3390/f14030469.

Moradi-Amirabad, Y., Rahimian, H., Babaeizad, V., & Denman, S. (2019). *Brenneria* spp. and *Rahnella victoriana* associated with acute oak decline symptoms on oak and hornbeam in Iran. *Forest Pathology*, 49(4), e12535.https://doi.org/10.1111/efp.12535.

Nechita, C., & Camarero, J. J. (2025). Hotter winter-spring droughts accelerated the growth decline of marginal pedunculate oak (*Quercus robur*) populations in dry sites from Romania. *Dendrochronologia*, 126369. https://doi.org/10.1016/j.dendro.2025.126369.

Oksanen, J., Blanchet, F. G., Friendly, M., Kindt, R., Legendre, P., McGlinn, D., *et al.* (2016). *vegan: Community Ecology Package* (R package version 2.4-1).

Oksanen, J., Blanchet, F. G., Kindt, R., Legendre, P., Minchin, P. R., O'hara, R. B., ... & Oksanen, M. J. (2013). Package 'vegan'. *Community ecology package, version*, *2*(9), 1-295.

Ou, X., Cao, J., Cheng, A., Peppelenbosch, M. P., & Pan, Q. (2019). Errors in transla-tional decoding: tRNA wobbling or misincorporation?. *PLoS genetics*, 15(3),

e1008017.https://doi.org/10.1371/journal.pgen.1008017.

Panahi, P., Jamzad, Z., Pourmajidian, M. R., Fallah, A., & Pourhashemi, M. (2012). Fo-liar epidermis morphology in Quercus (subgenus *Quercus*, section *Quercus*) in Iran. Acta Botanica Croatica, 71(1), 95-113.https://doi.org/10.2478/v10184-010-0029-y.

Rokhbakhsh-Zamin, F., Sachdev, D., Kazemi-Pour, N., Engineer, A., Pardesi, K. R., Zinjarde, S., ... & Chopade, B. A. (2011). Characterization of plant-growth-promoting traits of *Acinetobacter* species isolated from rhizosphere of *Pennisetum glaucum*. *Journal of Microbiology and Biotechnology*, 21(6), 556-566.https://doi.org/10.4014/jmb.1012.12006.

Sagheb Talebi, K., Sajedi, T., & Pourhashemi, M. (2014). Forests of Iran: A treasure from the past, a hope for the future. *Springer*. https://doi.org/10.1007/978-94-007-7371-4.

Sapp, M., Lewis, E., Moss, S., Barrett, B., Kirk, S., Elphinstone, J. G., & Denman, S. (2016). Metabarcoding of bacteria associated with the acute oak decline syndrome in England. *Forests*, 7(5), 95. https://doi.org/10.3390/f7050095.

Schaad, N. W., Jones, J. B., & Chun, W. (2001). *Laboratory guide for the identification of plant pathogenic bacteria* (3rd ed.). APS Press.

Sturz, A. V., Christie, B. R., Matheson, B. G., & Nowak, J. (1997). Biodiversity of endophytic bacteria which colonize red clover nodules, roots, stems and foliage and their influence on host growth. Biology and Fertility of Soils, 25, 13-19.https://doi.org/10.1007/s003740050273.

Taghimollaei, Y., & Karamshahi, A. (2017). Sudden Oak Death in Iran forests. *International Journal of Forest, Soil & Erosion*, *7*(1).

Trivedi, P., Spann, T., & Wang, N. (2011). Isolation and characterization of benefi-cial bacteria associated with citrus roots in Florida. Microbial ecology, 62, 324-336. https://doi.org/10.1007/s00248-011-9822-y.

Wakelin, S. A., Chu, G., Broos, K., Clarke, K. R., Liang, Y., & McLaughlin, M. J. (2010). Structural and functional response of soil microbiota to addition of plant substrate are moderated by soil Cu levels. Biology and Fertility of Soils, 46, 333-342. https://doi.org/10.1007/s00374-009-0436-1.

Zhang, N., Wang, Z., Shao, J., Xu, Z., Liu, Y., Xun, W., ... & Zhang, R. (2023). Biocontrol mechanisms of *Bacillus*: Improving the efficiency of green agriculture. *Microbial Biotechnology*, *16*(12), 2250-2263. https://doi.org/10.1111/1751-7915.14348.

Zhou, J., Bruns, M. A., & Tiedje, J. M. (1996). DNA recovery from soils of diverse composition. Applied and environmental microbiology, 62(2), 316-322. https://doi.org/10.1128/aem.62.2.316-322.1996.

Zolfaghari, R., Fayyaz, P., Dalvand, F., & Rezaei, R. (2024). The first report of *Quercus brantii* dieback caused by *Lelliottia nimipressuralis* in Zagros forests, Iran. Folia Forestalia Polonica. Series A. Forestry, 66(4).https://doi.org/10.2478/ffp-2024-0030.

How to cite this paper:

Ahmadi, E., Kowsari, M., Azadfar, D. and Salehi Jouzani, G. (2025). Polymicrobial Shifts in the Culturable Bacterial Microbiome Associated with Persian Oak Decline in West of Iran. *Microbiology, Metabolites and Biotechnology, 8*(2), 81-94.
DOI: 10.22104/mmb.2025.7777.1181